

1 **The frequency-following response (FFR) to speech stimuli: a normative dataset in**
2 **healthy newborns**

3
4
5 Teresa Ribas-Prats^{1,2,3}, Laura Almeida^{3,4}, Jordi Costa-Faidella^{1,2,3}, Montse Plana^{3,4}, MJ Corral^{1,2,3},
6 M. Dolores Gómez-Roig^{3,4}, Carles Escera^{1,2,3}

7
8 ¹ Brainlab – *Cognitive Neuroscience Research Group*. Department of Clinical Psychology and
9 Psychobiology, University of Barcelona (Catalonia-Spain)

10 ² Institute of Neurosciences, University of Barcelona (Catalonia-Spain)

11 ³ Institut de Recerca Sant Joan de Déu, Esplugues de Llobregat (Barcelona, Catalonia-Spain)

12 ⁴ BCNatal – Barcelona Center for Maternal Fetal and Neonatal Medicine (Hospital Sant Joan de
13 Déu and Hospital Clínic), University of Barcelona, Barcelona (Catalonia-Spain).

14
15
16
17 **Abbreviated title:** Normative FFR in neonates

18
19
20 ***Correspondence:** Carles Escera, PhD, Professor. Department of Clinical Psychology and
21 Psychobiology, University of Barcelona. Passeig de la Vall d'Hebron 171, 08035 Barcelona,
22 Catalonia-Spain. Tel: +34 933 125 048, Fax: +34 934 021 584, E-mail: cescera@ub.edu

23
24
25
26 Number of pages: 22; Number of words in Abstract: 197; Number of words in the manuscript:
27 8214. Number of figures: 8. Number of tables: 2.

28
29
30 **Declarations of interest:** none.

31 **Highlights**

- 32 • Frequency-following responses (FFR) were recorded on 46 newborns
- 33 • Seven objective FFR parameters were retrieved in time and frequency domains
- 34 • A normative data-base is offered to guide future clinical studies

35

36

37

38

39

40

41

42

43

44

45

46

47

48

49

50

51

52

53

54

55

56

57

58 **Abstract**

59 The Frequency-Following Response (FFR) is a neurophonic auditory evoked potential that
60 reflects the efficient encoding of speech sounds and is disrupted in a range of speech and
61 language disorders. This raises the possibility to use it as a potential biomarker for literacy
62 impairment. However, reference values for comparison with the normal population are not yet
63 established. The present study pursues the collection of a normative database depicting the
64 standard variability of the newborn FFR. FFRs were recorded to /da/ and /ga/ syllables in 46
65 neonates born at term. Seven parameters were retrieved in the time and frequency domains,
66 and analyzed for normality and differences between stimuli. A comprehensive normative
67 database of the newborn FFR is offered, with most parameters showing normal distributions
68 and similar robust responses for /da/ and /ga/ stimuli. This is the first normative database of the
69 FFR to characterize normal speech sound processing during the immediate postnatal days, and
70 corroborates the possibility to record the FFRs in neonates at the maternity hospital room. This
71 normative database constitutes the first step towards the detection of early FFR abnormalities
72 in newborns that would announce later language impairment, allowing early preventive
73 measures from the first days of life.

74 **Keywords:** auditory brainstem response, FFR, auditory processing, speech encoding, hearing
75 screening, human neonates, language impairments, cognition.

76

77 **1. Introduction**

78 Auditory brainstem responses (ABR) otoacoustic emissions (OAE) to simple auditory stimuli are
79 used in clinical practice to assess auditory pathway integrity (Hoth et al., 2009; Moller, 1999;
80 Stuart et al., 1996). Universal newborn hearing screening based on the ABR or OAE has provided
81 the earliest possible diagnosis for infants with permanent hearing loss (Moeller et al., 2006).
82 ABRs can also be elicited with more complex stimuli such as speech or music. Studying brainstem
83 responses to complex stimuli has revealed that the subcortical auditory system is more than a
84 set of relay stations transmitting information from the peripheral sensory epithelium to the
85 cerebral cortex (Song et al., 2008). Subcortical contributions to the neural representation of
86 sound can hence be reliably studied using a variant of the ABR, the so-called Frequency-
87 Following Response (FFR).

88 The FFR is a non-invasive electrophysiological measurement that reflects the encoding of the
89 temporal and spectral characteristics of complex evoking sounds in a cortico-subcortical
90 auditory network (Bidelman, 2018; Kraus and White-Schwoch, 2015; Skoe and Kraus, 2010).
91 Disruptions in the FFR are found in children with deficits in phonological awareness, reading and
92 abnormal timing resolution (Abrams et al., 2006; Banai et al., 2009, 2005; Basu et al., 2010;
93 Hornickel et al., 2012, 2011, 2009; Johnson et al., 2007; King et al., 2002; Kraus et al., 1996;
94 Wible et al., 2004). Children with reading or language disorders have significantly slower neural
95 response timing, weak neural encoding of formant-related stimulus harmonics and less robust
96 tracking of frequency contours than typically developing children (Banai et al., 2005; Basu et al.,
97 2010; Billiet and Bellis, 2010; Hornickel et al., 2009; Wible et al., 2004).

98 In addition, neurodevelopmental disorders characterized by impaired communication and
99 literacy skills such as dyslexia or autism spectrum disorder (ASD) have been associated with
100 abnormal subcortical representation of speech sounds. Hornickel and Kraus (2013) described
101 that children with dyslexia are characterized by delayed and harmonically impoverished
102 responses from the auditory brainstem (Banai et al., 2009; Basu et al., 2010; Hornickel et al.,
103 2012, 2011) and reduced subcortical representation of stimulus differences (Banai et al., 2005;
104 Hornickel et al., 2009). In children with ASD, Russo et al. (2009) reported deficits in timing and
105 frequency encoding of speech sounds at brainstem level. ASD individuals also exhibited a
106 subcortical neural response which was more vulnerable to background noise in comparison to
107 typically developing children. Another recent study described more variable FFRs in children
108 with ASD compared to their healthy peers (Otto-Meyer et al., 2018).

109 Moreover, White-Schwoch and colleagues (2015a) examined the FFRs recorded from a group of
110 3-4 years old children and reported that the precision and stability of the neural encoding of
111 consonants in noise predicted performance on reading readiness tests one year after the
112 neurophysiological assessment. In infants with ages between 3 to 10 months, Anderson et al.
113 (2015) found a robust fundamental frequency representation while the amplitudes of the first
114 formant and higher harmonics in the FFR increased with age. Thus, the FFR may offer a
115 neurophysiological marker of the efficient encoding of speech sounds related to literacy abilities
116 (Hornickel and Krauss, 2013).

117 In spite of the potential of the FFR to anticipate reading and literacy impairments, little is known
118 about the neural transcription of speech sounds in newborns. Recently, Kraus and

119 White-Schwoch (2016) suggested an idealized scenario where the FFR could be registered after
120 the hearing screening test was passed using the same equipment, with only replacing the
121 typical click or burst stimulus used for ABR with a speech sound. Their claim was that FFR
122 screening could help identifying newborns at risk of developing literacy impairments in the
123 future, so that they could be referred to appropriate specialists for a more exhaustive
124 examination.

125 The interest to improve our knowledge in the early maturation of complex sound processing at
126 brainstem level is further encouraged by the plasticity of neural tissues in subcortical structures
127 (Johnson et al., 2008; Krishnam et al., 2009, 2005; Musacchia et al., 2007; Russo et al., 2005;
128 Song et al., 2008; Strait et al., 2009; Wong et al., 2007). Recent studies have shown that the
129 FFR is sensitive to language (Krishnan et al., 2009, 2005; Krizman, 2015; Xu et al., 2006), musical
130 experience (Bidelman et al., 2014; Johnson et al., 2008; Lee et al., 2009; Musacchia et al., 2007;
131 Strait et al., 2009; Weiss and Bidelman, 2015; Wong et al., 2007) and short- and long-term
132 auditory adaptation and training (Escera, 2017; Russo et al., 2005; Song et al., 2008). Evidence
133 of brainstem response modulation by musical training has been shown with a few years of
134 lessons (Parbery-Clark et al., 2012; Strait and Kraus, 2014; Zuk et al., 2013) and observed in
135 very young musicians of 3 years of age (Skoe and Kraus, 2013; Strait et al., 2014, 2013, 2012).
136 After a revision of a number of phonologic intervention studies, Handler et al. (2011) confirmed
137 the effectiveness of phonologic training implementation during the first years of life in reading
138 impaired children as compared to those who were not identified or helped until years later
139 (Foorman et al., 2003; Lyon et al., 2010; National Institutes of Health, 2000; Schatschneider
140 and Torgesen, 2004; Vellutino et al., 2004; Willcutt and Pennington, 2000). Hence, detecting
141 early FFR abnormalities in newborns that would announce later language impairment would
142 allow installing early preventive measures such as music enrichment programs (Kraus et al.,
143 2014).

144 The possibility to record FFR in newborns has been suggested in no more than ten studies so
145 far, showing a remarkable similarity between the adult and newborn responses (Gardi et al.,
146 1979; Jeng et al., 2016, 2013, 2011b). In addition, Jeng et al. (2016, 2013, 2011b) reported
147 similar FFRs in American and Chinese newborns indicating an early and universal maturation of
148 voice-pitch processing at brainstem level in neonates at 1-3 days after birth. However, before
149 the FFR can be used in the clinics, normative values need to be established. The aim of the
150 present study was the collection of a normative database depicting the standard variability
151 observed in different relevant parameters retrieved from the newborn FFR.

152

153 **2. Methods**

154 *2.1. Participants*

155 Fifty term newborns (24 females, aged 14-125 hours after birth) were recruited from *Sant Joan*
156 *de Déu Hospital* in Barcelona (Catalonia, Spain). By medical reports, all newborns were low-risk
157 gestations without neither obstetric pathologies nor risks factors for hearing impairment as
158 determined by the Committee on Infant Hearing as a “high-risk registry” (Joint Committee on
159 Infant Hearing, 1994). All the participants had a high Apgar score (>7) at 1 and 5 minutes of life.

160 All newborns passed the standardized hearing screening of peripheral auditory health using an
161 automated auditory brainstem response system (ALGO 3i, Natus Medical Incorporated, San

162 Carlos, CA), before the experiment. Each newborn also passed a normal click-evoked auditory
163 brainstem response collected with a standard SmartEP platform (Intelligent Hearing Systems,
164 Miami, FL). Standard click ABR was recorded in response to a 100 μ s square-wave click stimulus
165 presented at 55 dB SPL according to standard procedures to the Joint Committee on Infant
166 Hearing (2007). Mean latency and amplitude of wave V were 8.90 (\pm 0.79 SD) ms and 0.27 (\pm
167 0.15 SD) μ V, respectively (Fig. 1), being comparable to the norms published by Stuart et al.
168 (1994). Four newborns were excluded from the final sample because their wave V could not be
169 reliably identified.

170 Informed consent was obtained from legal guardians of the newborns assessed in accordance
171 with the Declaration of Helsinki after the study has approved by the Ethical Committee of Clinical
172 Research (CEIC) of the Sant Joan de Déu Foundation.

173 2.2. Stimuli

174 The complex auditory stimuli used were the syllables /da/ and /ga/ created with a Klatt-based
175 synthesizer (Klatt, 1976) and modified by Praat (Boersma and Weenink, 2013) to have a
176 fundamental frequency (F_0) of 113 Hz in both syllables. The use of F_0 of 113 Hz instead of the
177 very common F_0 at 100 Hz was motivated to avoid contamination by harmonics of the 50 Hz
178 electric line in Europe. The stimuli had a duration of 170 ms, including a 10 ms onset period, a
179 47 ms consonant transition and a 113 ms steady state vowel. These sounds differed only by the
180 trajectory of their second formant (F_2) during the consonant transition (/da/: 1438-1214 Hz;
181 /ga/: 1801-1214 Hz). In the vowel region, all the formants were stable in both syllables. Stimuli
182 were presented at 55 dB SPL in alternating polarities with a 100.27 ms inter-stimulus interval
183 (presentation rate of 3.7 Hz) to the right ear through Etymotic shielded earphones of 300 ohms
184 (ER, Elk Grove Village, IL, EEUU) connected to Flexicoupler[®] (Natus Medical Incorporated, San
185 Carlos, CA) adaptor.

186 2.3. Procedure

187 All newborns were tested in the hospital room where they were resting with their mother once
188 the newborn hearing screening was already passed. For the recording, each newborn was asleep
189 in its own bassinet and the researcher interrupted the experiment to any sign of sleep
190 disruption, to restart the recording as soon as the newborn was calm again. The total mean
191 duration of a test session was 26.09 (\pm 3.56 SD) min (51.81 ms x 2000 sweeps x 1 condition +
192 270.27 ms x 2000 sweeps x 2 conditions + duration of sweeps rejected + time needed to check
193 electrodes impedances + time for the newborn restored the sleep in case that it was disrupted).
194 If the recording time exceeded this duration, the session was canceled and postponed for several
195 hours or until the next day.

196 2.4. Data acquisition

197 FFRs were collected with a SmartEP platform including the *cABR* and *Advanced Hearing Research*
198 modules (Intelligent Hearing Systems, Miami, FL, EEUU). Auditory brainstem responses to click
199 and to the syllables /da/ and /ga/ were recorded using disposable snap Ag/AgCl electrodes
200 placed in a vertical montage (the active electrode was located at Fpz, references at each ear,
201 and ground at the forehead) with impedances < 5 k Ω (Fig. 2). Only the ipsilateral reference was
202 used in the analysis (Hornickel et al., 2009). The continuous EEG was online bandpass filtered

203 from 30-3000 Hz and acquired with a sampling rate of 13333 Hz. Responses were collected by
204 alternating polarity and averaged $((\text{Org.} + \text{Inv.})/2)$ to isolate the neural response by minimizing
205 stimulus artifact and cochlear microphonic (Aiken and Picton, 2008). Any activity exceeding ± 30
206 μV was rejected online as an artifact, and a total of 2000 artifact-free responses were averaged
207 for each syllable and newborn. Rejection was smaller than 15% of sweeps per condition.

208 *2.5. Data processing and analyses*

209 Neural responses to /da/ and /ga/ were averaged separately and epoched into 270.27 ms
210 windows (including 40 ms pre-stimulus period). After averaging, data were filtered off-line with
211 a spectral bandpass filter with infinite slope from 80 to 3000 Hz to isolate brainstem responses
212 (Chandrasekaran and Kraus, 2009).

213 After a review of the analytic techniques used to characterize the FFR in different populations
214 (Anderson et al., 2015; Banai et al., 2009; Basu et al., 2010; Hornickel et al., 2012, 2011, 2009;
215 Hornickel and Kraus, 2013; Jeng et al., 2013, 2011a, 2011b, 2010; Jonhson et al., 2008, 2007; Liu
216 et al., 2015; Musacchia et al. 2007; Neef et al., 2017; Russo et al., 2005; 2004; Skoe et al., 2011;
217 Strait et al., 2014; White-Schwoch et al., 2015a and 2015b; White-Schwoch and Kraus, 2013), an
218 extensive number of parameters are included in this study to offer an accurate description of
219 FFR properties in newborns. In the time domain, cross-correlation between the stimulus and the
220 neural response, the neural lag and the signal-to-noise ratio (SNR) are reported. Pitch error and
221 pitch strength, extracted from a sliding time-window autocorrelation approach, were also
222 evaluated. In the spectral domain, the amplitude of the fundamental frequency and its
223 harmonics was calculated based on fixed time-windows. Signal-to-noise ratio variation along the
224 stimulus duration, computed as points below noise floor using a sliding time-window approach,
225 is also reported. All analyses were performed under Matlab R2015b (Mathworks) using routines
226 provided by Intelligent Hearing Systems (Miami, FL, EEUU) and custom scripts developed in our
227 laboratory. The following sections describe the rationale and procedure to obtain each of these
228 measures.

229 *2.5.1. Time domain*

230 To examine the FFR in the time domain, a cross-correlation between each syllable stimulus and
231 the neural response was computed. For the purpose of comparison, each syllable was resampled
232 to the sampling rate of the EEG recording (13333 Hz), and bandpass filtered between 80 – 3000
233 Hz. The magnitude of the first maximum cross-correlation peak and its lag are reported. In
234 addition, the signal-to-noise ratio (SNR) of the FFR was computed in three time windows,
235 corresponding to three different regions of the acoustic stimulus: consonant transition (10 – 57
236 ms), vowel (57 – 170 ms) and entire response (0 – 170 ms). In the following lines, each of these
237 objective parameters is briefly described.

238 *2.5.1.1. Stimulus-to-response cross-correlation.* The cross-correlation magnitude shows how
239 faithfully the FFR reproduces the stimulus waveform as a function of the time shift between the
240 two (Russo et al., 2004). The maximum cross-correlation value was obtained within a response
241 time lag of 3 to 10 ms, in line with previous studies (Jeng et al., 2010).

242 2.5.1.2. *Neural lag*. The neural lag is an estimation of the transmission delay between stimulus
243 and response. It was retrieved as the time lag that produced the maximum stimulus-to-response
244 cross-correlation magnitude computed as described above.

245 2.5.1.3. *Signal-to-noise ratio (SNR)*. Root mean square (RMS) amplitude (in μV) indicates the
246 overall magnitude of neural activity over time (Liu et al., 2015). RMS is calculated by squaring
247 each point in a region of the response waveform, computing the mean of the squared values
248 and then computing its square root. The RMS amplitudes of the FFR to the consonant transition,
249 the vowel and the entire stimulus were computed separately and divided by the RMS amplitude
250 of the pre-stimulus period (-40 – 0 ms) (Anderson et al., 2015; Russo et al., 2004). In order to
251 account for individual response-to-stimulus delays, the individual neural lag retrieved from the
252 stimulus-response cross-correlation analysis was added to each of the selected regions (except
253 to the pre-stimulus region).

254 Additionally, we computed the autocorrelation function of the entire FFR recording in a sliding
255 time-window approach, using short bins of 40 ms (Hanning tapered) with 1 ms step size. In each
256 bin, the periodicity of the F_0 was estimated as the frequency (inverse of the lag) yielding the
257 maximum autocorrelation value (Boersma, 1993) within a predefined frequency range, fixed
258 from 103 to 123 Hz, leaving a 10 Hz buffer at each side of the F_0 frequency of the stimulus (113
259 Hz) (Jeng et al., 2013, 2011b, 2010). The F_0 s from each bin were concatenated to construct the
260 F_0 contour of the FFR recording. The same procedure was applied to the stimulus waveforms
261 /da/ and /ga/. Two objective parameters were extracted using this method, as described next.

262 2.5.1.4. *Pitch error*. Pitch error (in Hz) is a measure of pitch encoding accuracy of the FFR along
263 the syllable presentation. Once the syllable was shifted the time equivalent to the average of
264 the individual neural lag, the absolute Euclidian distance between the syllable F_0 and the
265 response F_0 from each bin was calculated and averaged together (Liu et al., 2015; Song et al.,
266 2008).

267 2.5.1.5. *Pitch strength*. Pitch strength is a measure of periodicity that reflects the robustness of
268 the response's phase-locking to the syllable F_0 contour (Jeng et al, 2013). It was computed as the
269 average across bins of the normalized autocorrelation values at the signal's F_0 .

270 2.5.2. *Frequency domain*

271 To examine the FFR in the frequency domain, we computed a Fast Fourier Transform (FFT;
272 Hamming windowed) separately for the three different regions of the stimuli as described above
273 (see 2.5.1), each region adjusted for each newborn to account for the individual neural lag. In
274 order to avoid artifact differences in power estimates due to different window lengths, the
275 Welch's averaging method (Welch, 1967; *pwelch.m* Matlab function) was applied to estimate
276 the power spectrum of the demeaned signal corresponding to the consonant transition, the
277 vowel and the entire response (segments of 40 ms, equivalent to the window length of the pre-
278 stimulus region; Hamming windowed; 82.5% overlap; spectrum type specified as 'power').

279 2.5.2.1. *Spectral amplitude*. The spectral amplitude indicates the magnitude of neural
280 phaselocking at a certain frequency (White-Schwoch et al., 2015b). In order to compare our
281 results with the previous literature, a square root of power estimates was applied to convert
282 them to spectral amplitude. Spectral amplitude corresponding to the F_0 (113 Hz) and its integer

283 harmonics up to 1500 Hz (i.e., HH₂₋₁₃) were computed as the mean over a ± 5 Hz frequency
284 window centered at each individual peak. Two values are reported: 1) the F₀ spectral amplitude;
285 and 2) a composite value for all F₀ harmonics, resulting from averaging the spectral amplitudes
286 of HH₂₋₁₃ (Krizman et al., 2015; Parbery-Clark et al., 2009).

287 *2.5.2.2. Points below noise floor.* In addition, we computed the spectrogram of the entire FFR
288 recording in short bins of 40 ms (Hanning tapered) with 1 ms step size. Spectral amplitudes were
289 computed with FFTs after zero-padding each FFR bin to 1s to increase spectral resolution, and
290 Hanning windowed. This method allowed extracting the points below noise floor, which is an
291 objective index that describes how the signal could be discerned and differentiated from the
292 noise. It is computed dividing the F₀ spectral amplitude of each bin by the F₀ spectral amplitude
293 computed in the pre-stimulus region (Song et al., 2008). The total number of bins in which the
294 spectral amplitude of F₀ is smaller in the post- vs. the pre-stimulus region is reported.

295 *2.6. Statistical analyses*

296 SPSS 22.0 was used for statistical analysis. Descriptive statistics for each parameter computed
297 for each syllable (/da/, /ga/) are presented as mean and standard deviation (SD) or median and
298 interquartile range (IQR), after assessing normality distribution by Kolmogorov-Smirnov Statistic
299 with Lilliefors' Significance.

300 The initial statistical approach was a 2x2 repeated measures analysis of variance (RMANOVA),
301 with syllable (/da/, /ga/) and region (consonant transition, vowel) as factors. However, in the
302 objective indices where the results were obtained only in one response region (i.e., stimulus-to-
303 response cross-correlation, neural lag, pre-stimulus RMS amplitude, pitch error, pitch strength
304 and points below noise floor), a t-test or Wilcoxon test was computed according to the
305 assumption of normal distribution. In the spectral amplitude analyses, a third factor was
306 included (harmonic: F₀, average amplitude HH₂₋₁₃). The Greenhouse–Geisser correction was
307 applied when the assumption of sphericity was violated. A result was considered significant
308 when $p < 0.05$ using a two-tailed analysis. Bonferroni correction was used to adjust p-values for
309 all multiple pairwise contrasts.

310 **3. Results**

311 Grand-average FFR waveforms for both syllables (/da/, /ga/) and the corresponding amplitude
312 spectra of the consonant transition and the vowel regions of the response are shown in Fig. 3A.
313 Individual waveforms and corresponding amplitude spectra from a typical newborn with high
314 SNR (NF 029) and from another newborn with very low SNR (NF 038) are plotted in Fig. 3B and
315 3C, respectively. Grand-average spectrograms are presented in Fig. 4A, and those from the same
316 individual newborns as in Fig. 3 are shown in Fig. 4B and 4C. As Fig. 4 shows, the newborn FFR
317 contains clear energetic content in the F₀ contour of the syllable, but not in its harmonic
318 frequencies, in agreement with Jeng et al. (2016, 2013, 2011b). Below, we provide a series of
319 descriptive statistics extracted from the values obtained to all computed parameters. In
320 addition, we provide a statistical comparison of parameter values across stimulus types (syllable
321 /da/ vs. /ga/).

322 *3.1. Time domain*

323 In the time domain, a normal distribution was observed for most of the parameters assessed.
324 Only the values of the SNR computed for the consonant transition when the syllable /da/ was
325 presented and the values of the SNR calculated for the vowel and the entire response when the
326 syllable /ga/ was presented did not follow a normal distribution. The corresponding descriptive
327 statistics are reported in Table 1. Fig. 5 illustrates the distribution of the values obtained in all
328 time-domain parameters for each syllable (/da/, /ga/) and indicates the response region
329 assessed (consonant transition and vowel) for SNR. Pitch tracking and pitch strength obtained
330 from the grand-average waveforms and from the individual newborns depicted in Fig. 3 with
331 high and low SNR are shown in Fig. 6 and 7, respectively.

332 A comparison of the time-domain parameter values obtained to the /da/ and /ga/ syllables
333 showed no significance differences in stimulus-to-response cross-correlation values ($t(45) =$
334 $0.032, p = 0.974$) nor in neural lag ($t(45) = -0.251, p = 0.803$). RMS amplitudes during the pre-
335 stimulus baseline period were not significantly different either ($t(45) = 1.860, p = 0.069$). Thus,
336 any difference observed in response to the /da/ and /ga/ stimuli could not be attributed to
337 variation in pre-stimulus spontaneous activity. However, no differences were observed in SNR
338 between syllables ($F(1,45) = 1.630, p = 0.208, \eta^2 = 0.239$). Regarding response region, in contrast
339 with previous studies, the SNR of the vowel was smaller than that of the consonant transition,
340 irrespective of the syllable ($F(1,45) = 32.385, p < 0.001, \eta^2 = 1$). Finally, pitch measurements,
341 extracted from a sliding time-window autocorrelation approach applied to the entire FFR
342 recording, did not show any significant differences between syllables either (pitch error: $t(45) =$
343 $-1.440, p = 0.157$; pitch strength: $t(45) = -1.187, p = 0.242$).

344 3.2. Frequency domain

345 In the frequency domain, spectral amplitude values followed a normal distribution for most of
346 the conditions assessed. However, points below noise floor values did not pass the Kolmogorov-
347 Smirnov test. Descriptive statistics are reported in Table 2. Fig. 8 illustrates the distribution of
348 spectral amplitude values across response regions (consonant transition, vowel), harmonics ($F_0,$
349 HH_{2-13}) and syllables (/da/, /ga/), as well as the distribution of points below noise floor values
350 across syllables. Fig. 6 shows the points below noise floor computed from the grand-average
351 waveforms and from the individual newborns depicted in Fig. 3 with high and low SNR.

352 A three-factor RMANOVA (syllable: /da/, /ga/; region: consonant transition, vowel; harmonic:
353 F_0, HH_{2-13}) performed on all spectral amplitude values showed no significance differences
354 between syllables ($F(1,45) = 0.038, p = 0.846, \eta^2 = 0.054$). Regarding response region, spectral
355 amplitudes were larger to the consonant transition than to the vowel ($F(1,45) = 22.008, p <$
356 $0.001, \eta^2 = 0.996$) in agreement with previous studies (White-Schwoch et al., 2015b). Regarding
357 the harmonic factor, an expected significant effect was found in spectral amplitude ($F(1,45) =$
358 $274.123, p < 0.001, \eta^2 = 1$), being larger for the F_0 than for its harmonics. A significant interaction
359 between the region and the harmonic was observed as well ($F(1,45) = 23.631, p < 0.001, \eta^2 =$
360 0.997). Post-hoc analyses showed a slightly higher difference in spectral amplitudes between
361 the F_0 and those of the HH_{2-13} in the consonant transition (mean $F_0 = 43.293$ nV, SE = 2.801; mean
362 $HH_{2-13} = 2.892$ nV, SE = 0.110) than in the vowel portion (mean $F_0 = 35.212$ nV, SE = 1.902; mean
363 $HH_{2-13} = 2.917$ nV, SE = 0.101). Finally, no significant differences were observed in points below
364 noise floor across syllables ($Z = -1.116, p = 0.264$).

365 **4. Discussion**

366 We here provide the first normative database of the newborn FFR, thus demonstrating the
367 feasibility to record this electrophysiological response from bedside, in the maternity unit where
368 newborns are delivered, during their first hours of life.

369 In order to obtain a comprehensive database, two syllables with different stop consonants (/da/
370 /ga/) were presented to 50 newborns aged 14-125 hours. Descriptive statistics of each of the
371 parameters assessed were obtained (see Table 1-2). Normal distribution was confirmed for most
372 of them, for which mean and standard deviation are reported. In those cases in which parameter
373 values did not follow a normal distribution, median and interquartile range are reported instead.
374 The representation of the distribution of all values using quartiles opens the possibility to
375 determine the location of an individual's scores and to assess if her/his results are included into
376 the central 50% of values. In general, comparing our results with previous literature, we found
377 smaller values in all measures (Skoe et al., 2013; Strait et al., 2013; White-Schwoch et al., 2015b)
378 except in pitch error and pitch strength (Jeng et al., 2010). The lower values obtained, according
379 to Skoe et al. (2013) could be attributed to age differences.

380 For each of the objective parameters assessed, no differences between /da/ and /ga/ syllables
381 were observed, indicating that these two stimuli could be used interchangeably to obtain a
382 potential snapshot of pitch representation in the newborn's brain before they are discharged.
383 However, differences were found between parameter values extracted from distinct portions of
384 the FFR, which corresponded to different stimulus regions, and from different harmonic
385 components of the frequency spectrum. For instance, higher SNR and spectral amplitude values
386 were found in the consonant transition compared to the vowel, possibly due to response
387 adaptation. In contrast, White-Schwoch et al. (2015b) showed higher SNR values for the vowel
388 region than for the consonant transition, although comparable results in spectral amplitude.
389 Regarding the harmonic content, higher spectral amplitude values were observed for the F_0 in
390 comparison to higher harmonics (see Fig. 8), in line with previous observations (Anderson et al.,
391 2015; Banai et al., 2009; Jeng et al., 2016, 2013, 2011b; White-Schwoch et al., 2015b). While we
392 cannot rule out that this may be a particular characteristic of the newborn FFR, the procedure
393 used to obtain it, by averaging responses to opposite polarities, may have exerted a major
394 influence. In fact, while this operation enhances envelope representation, which is not polarity
395 dependent, it eliminates the temporal fine structure of the signal, drastically reducing the
396 spectral energy of the present harmonics (Aiken and Picton, 2008). This explanation may
397 account as well for the lack of differences found in parameter values across syllables.

398
399 The results obtained here are in line with those of Jeng and colleagues (2016, 2013, 2011b) who
400 corroborated that the newborn FFR (age: 1-3 days) could be registered during the first days of
401 life (Gardi et al., 1979). In addition to finding evident spectral energy content at the F_0 in the
402 newborn FFR spectrograms, differences in the F_0 spectral energetic content across the individual
403 newborns assessed were observed (Jeng et al., 2016, 2013, 2011b), as in our study. However,
404 descriptive statistics of the different FFR parameters as the ones computed in the present study
405 were only published in Jeng et al. (2010), specifically for measurements related to pitch tracking.
406 They found similar FFRs to voice pitch between infants of 5.7 months mean age and adults using
407 a Chinese monosyllabic stimulus that mimics the English vowel /i/ with a rising pitch (117 to 166

408 Hz). Mean and standard deviation of pitch error and pitch strength recorded from the infant
409 group were slightly smaller than those found in the present study. In spite of the differences in
410 group age and the stimulus materials, our results, together with those of Jeng et al. (2010),
411 confirm that pitch is accurately processed during the first stages of life.

412

413 We believe our study contributes a step forward towards achieving the ideal scenario proposed
414 by Kraus and White-Schwoch (2016). Taking the universal newborn hearing screening (UNHS) as
415 a reference, they proposed the implementation of a cognitive screening after the UNHS is
416 passed, by using the same recording system where only the classical click stimulus would be
417 replaced by a speech sound. In this study, FFRs were recorded in the hospital room where
418 newborns were resting with their mothers after the auditory screening was passed. Auditory
419 pathway integrity was corroborated by Wave V identification to a click presentation (Fig. 1) using
420 the same portable equipment employed afterwards to record the FFR to the syllables /da/ and
421 /ga/. As the specific hearing screening protocol recommended by the Joint Committee of Infant
422 hearing (2007) to promote the early identification and intervention of children with hearing loss,
423 we suggest, according to Kraus and White-Schwoch (2016), the establishment of a protocol with
424 which the identification of a disrupted newborn FFR would prompt the child to be referred to a
425 coordinated team for follow up, in seeking intervention strategies to improve his/her literacy
426 abilities. Several studies support that spectro-temporal encoding mechanisms could be
427 improved after short- (Song et al., 2012) and long-term (Hornickel et al., 2012) training protocols
428 using the FFR as a fingerprint reflecting these improvements. The neural plasticity of the
429 subcortical auditory system during the first days of life highlights the importance to this period
430 to detect as earlier as possible an abnormal FFR.

431 The speech tokens selected (/da/ and /ga/) are extensively used in the literature because several
432 studies suggest that stop consonants are an important constraint in populations with literacy
433 impairments (Kraus et al., 1996; Tallal and Stark, 1981; Turner et al., 1992). However, recent
434 studies suggest that the identification of the speech in noise is especially compromised in
435 populations with specific language impairment (Cunningham et al., 2001; Hornickel et al., 2009,
436 White-Schwoch et al., 2015a, 2015b, 2013). To complement the present normative database,
437 future studies using different stimulus materials, for example including speech in noise, and
438 achieving other potential objective indices retrieved from the FFR are needed.

439 In any case, this study offers valuable information relative to a specific lifetime that was not
440 included in previous normative database research and remained to be described. Skoe and
441 colleagues (2013) characterized the auditory brainstem response of 586 healthy participants
442 across an extensive age range (from 3 months to 72 years). With our data we contribute to fill
443 the gap in the research focused on the FFR trends along the lifetime. In addition, an age-
444 appropriate normative database is critical to establish a reference with which to compare the
445 results of an individual from a population that presents risk factors to develop literacy
446 impairments (Jeng et al., 2016; Skoe et al., 2013).

447 Albeit the potential clinical utility attributed to the FFR, its small amplitude at the scalp in
448 contrast with the high background noise constraints the quality of the recordings to translate
449 the use of the FFR from brain research to clinical applications. The averaging method is usually
450 used in clinical practice to assess how the signal is discernible to the noise recorded as a function

451 of the number of sweeps presented (Jeng et al., 2011a). Recent studies offered different
452 threshold criterion depending on the statistical approach used and population assessed
453 (Bidelman et al., 2018, 2014; Jeng et al., 2018, 2013, 2011a). Thus, before the FFR could be
454 considered a universal clinical test, a consistent predetermined threshold to verify a
455 distinguishable FFR is required for each specific lifetime (Jeng et al., 2016).

456 In summary, the present study shows the possibility to record newborn FFR during the first
457 postnatal hours at the maternity unit before discharge and contributes to approximate the FFR
458 to clinical context. In agreement with Jeng et al. (2016), our study promotes longitudinal
459 research in which the newborns that present normal and abnormal FFR were followed up to
460 elucidate whether an FFR recorded during the first days of life could become a biomarker to
461 prevent future literacy disorders.

462

463 **Acknowledgements.**

464 The authors want to express their warmest thanks to all newborns that peacefully slept in their
465 basinet during our recordings, and to their mothers who generously agreed to participate in the
466 study. Also thanks go for Francisco Díaz-Santaella for inestimable technical support in
467 developing the scripts for data analysis. This work was supported by the 2017SGR-974 Excellence
468 Research Group of the Generalitat de Catalunya, the PSI2015-63664-P project (MINECO/FEDER),
469 and the ICREA Acadèmia Distinguished Professorship awarded to Carles Escera.

470 **References**

- 471 Abrams, D.A., Nicol, T., Zecker, S.G., Kraus, N., 2006. Auditory brainstem timing predicts cerebral
472 dominance for speech sounds. *J Neurosci.* 26, 11131–11137.
- 473 Aiken, S.J., Picton, T.W., 2008. Envelope and spectral frequency-following responses to vowel
474 sounds. *Hear Res.* 245, 35–47.
- 475 American Academy of Pediatrics, Joint Committee on Infant Hearing, 2007. Year 2007 Position
476 Statement: Principles and Guidelines for Early Hearing Detection and Intervention
477 Programs. *Pediatrics* 120, 898 - 921.
- 478 Anderson, S., Parbery-Clark, A., White-Schwoch, T. Kraus, N., 2015. Development of subcortical
479 speech representation in human infants. *J Acoust Soc Am.* 137, 3346–3355.
- 480 Banai, K., Hornickel, J., Skoe, E., Nicol, T., Zecker, S., Kraus, N., 2009. Reading and subcortical
481 auditory function. *Cereb Cortex.* 19, 2699–2707.
- 482 Banai, K., Nicol, T., Zecker, S.G., Kraus, N., 2005. Brainstem Timing: Implications for Cortical
483 Processing and Literacy. *J Neurosci.* 25, 9850–9857.
- 484 Basu, M., Krishnan, A., Weber-Fox, C., 2010. Brainstem correlates of temporal auditory
485 processing in children with specific language impairment. *Dev Sci.* 13, 77–91.
- 486 Bidelman, G. M., 2018. Subcortical sources dominate the neuroelectric auditory frequency-
487 following response to speech. *NeuroImage* 175, 56-69
- 488 Bidelman, G.M., Weiss, M.W., Moreno, S., Alain, C., 2014. Coordinated plasticity in brainstem
489 and auditory cortex contributes to enhanced categorical speech perception in
490 musicians. *Eur J Neurosci.* 40, 2662–2673.
- 491 Billiet, C.R., Bellis, T.J., 2010. The relationship between brainstem temporal processing and
492 performance on tests of central auditory function in children with reading disorders. *J*
493 *Speech Lang Hear Res.* 54, 228-242.
- 494 Boersma, P., 1993. Accurate short-term analysis of the fundamental frequency and the
495 harmonics-to-noise ratio of a sampled sound. *IFA Proceedings* 17, 97–110.
- 496 Boersma, P., Weenink, D., 2013. Praat: doing phonetics by computer [Computer program].
497 Version 5.3.51, retrieved 2 June 2013 from <http://www.praat.org/>.
- 498 Chandrasekaran, B., Kraus, N., 2009. The scalp-recorded brainstem response to speech: neural
499 origins and plasticity. *Psychophysiology* 47, 236-246.
- 500 Cunningham, J., Nicol, T., Zecker, S., Kraus, N., 2001. Neurobiologic responses to speech in noise
501 in children with learning problems: deficits and strategies for improvement. *Clin*
502 *Neurophysiol.* 112, 758-767.
- 503 Escera, C., 2017. The Role of the Auditory Brainstem in Regularity Encoding and Deviance
504 Detection. In: Kraus N, Anderson S, White-Schwoch T, Fay R and Popper A, editors. *The*
505 *Frequency Following Response: A Window into Human Communication.* Springer
506 International Publishing.
- 507 Foorman, B.R, Breier, J.I., Fletcher, J.M., 2003. Interventions aimed at improving reading
508 success: an evidence-based approach. *Dev Neuropsychol.* 24, 613– 639.

- 509 Gardi, J., Salamy, A., Mendelson, T., 1979. Scalp-recorded frequency-following responses in
510 neonates. *Audiology* 18, 494–506.
- 511 Handler, S.M. Fierson W.M., Section on Ophthalmology; Council on Children with Disabilities;
512 American Academy of Ophthalmology; American Association for Pediatric
513 Ophthalmology and Strabismus; American Association of Certified Orthoptists.,
514 2011. Learning disabilities, dyslexia, and vision. *Pediatrics* 127, 818 – 856.
- 515 Hornickel, J., Chandrasekaran, B., Zecker, S., Kraus, N., 2011. Auditory brainstem measures
516 predict reading and speech-in-noise perception in schoolaged children. *Behav Brain*
517 *Res.* 216, 597–605.
- 518 Hornickel, J., Kraus, N., 2013. Unstable representation of sound: a biological marker of dyslexia.
519 *J Neurosci.* 33, 3500–3504.
- 520 Hornickel, J., Skoe, E., Nicol, T., Zecker, S., Kraus, N., 2009. Subcortical differentiation of stop
521 consonants relates to reading and speech-in-noise perception. *Proc Natl Acad Sci U S A.*
522 106, 13022–13027.
- 523 Hornickel, J., Anderson, S., Skoe, E., Yi, H.G., Kraus, N., 2012. Subcortical representation of
524 speech fine structure relates to reading ability. *Neuroreport* 23, 6–9.
- 525 Hoth, S., Neumann, K., Weisschuh, H., Bräunert, J., Böttcher, P., Hornberger, C., Maul, H.,
526 Beedgen, B., Buschmann, K., Sohn, C., Hoffmann, G., Plinkert, P. (2009). Universal
527 newborn hearing screening. Methodical aspects. *HNO*, 57,29-36.
- 528 Jeng, F.C. Nance, B., Montgomery-Reagan, K., Lin C.D., 2018. Exponential modeling of
529 frequency-following responses in American neonates and adults. *J Am Acad Audiol.* 29,
530 125-134.
- 531 Jeng, F.C., Hu, J., Dickman, B., Lin, C.Y., Lin, C.D., Wang, C.Y., Chung, H.K., Li, X., 2011a. Evaluation
532 of two algorithms for detecting human frequency-following responses to voice pitch.
533 *Int J Audiol.* 50, 14–26.
- 534 Jeng, F.C., Hu, J., Dickman, B.M., Montgomery-Reagan, K., Tong, M., Wu, G., Lin, C.D., 2011b.
535 Cross-linguistic comparison of frequency-following responses to voice pitch in American
536 and Chinese neonates and adults. *Ear Hear.* 32, 699–707.
- 537 Jeng, F.C., Lin, C.D., Wang, T.C., 2016. Subcortical neural representation to Mandarin pitch
538 contours in American and Chinese newborns. *J Acoust Soc Am.* 139, 190-195.
- 539 Jeng, F.C., Peris, K.S., Hu, J., Lin, C.D., 2013. Evaluation of an automated procedure for detecting
540 frequency-following responses in American and Chinese neonates. *Percept Mot Skills.*
541 116, 456–465.
- 542 Jeng, F.C., Schnabel, E.A., Dickman, B.M., Hu, J., Li, X., Lin, C.D., Chung, H.K., 2010. Early
543 maturation of frequency-following responses to voice pitch in infants with normal
544 hearing. *Percept Mot Skills.* 111, 765–784.
- 545 Johnson, K., Nicol, T., Zecker, S.G., Kraus, N., 2007. Auditory brainstem correlates of perceptual
546 timing deficits. *J Cogn Neurosci.* 19, 376–385.
- 547 Johnson, K.L., Nicol, T., Zecker, S.G., Kraus, N., 2008. Developmental plasticity in the human
548 auditory brainstem. *J Neurosci.* 28, 4000–4007.

549 King, C., Warrier, C.M., Hayes, E., Kraus, N., 2002. Deficits in auditory brainstem encoding of
550 speech sounds in children with learning problems. *Neurosci Lett.* 319, 111–115.

551 Klatt, D., 1976. Software for cascade/parallel formant synthesizer. *J Acoust Soc Am.* 67, 971–
552 975.

553 Kraus, N., McGee, T., Carrell, T.D., Zecker, S.G., Nicol, T.G., Koch, D.B., 1996. Auditory
554 Neurophysiologic Responses and Discrimination Deficits in Children with Learning
555 Problems. *Science* 273, 971–973.

556 Kraus, N., Slater, J., Thompson, E.C., Hornickel, J., Strait, D.L., Nicol, T., White-Schwoch, T.,
557 2014. Auditory learning through active engagement with sound: Biological impact of
558 community music lessons in at-risk children. *Front Neurosci.* 8, 1-12.

559 Kraus, N., White-Schwoch, T., 2015. Unraveling the Biology of Auditory Learning: A Cognitive-
560 Sensorimotor-Reward Framework. *Trends Cogn Sci.* 19, 642-654.

561 Kraus, N., White-Schwoch, T., 2016. Newborn Hearing Screening 2.0. *Hear J.* 69, 44-45.

562 Krishnan, A., Swaminathan, J., Gandour, J., 2009. Experience-dependent enhancement of
563 linguistic pitch representation in the brainstem is not specific to a speech context. *J*
564 *Cogn Neurosci.* 21, 1092–1105.

565 Krishnan, A., Xu, Y., Gandour, J.T., Cariani, P.A., 2005. Encoding of pitch in the human brainstem
566 is sensitive to language experience. *Brain Res Cogn Brain Res.* 25, 161–168.

567 Krizman, J., Slatara, J., Skoe, E., Marian, V., Kraus, N., 2015. Neural processing of speech in
568 children is influenced by extent of bilingual experience. *Neurosci Lett.* 585, 48-53.

569 Lee, K.M., Skoe, E., Kraus, N., Ashley, R., 2009. Selective subcortical enhancement of musical
570 intervals in musicians. *J Neurosci.* 29, 5832-5840.

571 Liu, F., Maggu, A.R., Lau, J., Wong, P., 2015. Brainstem encoding of speech and musical stimuli
572 in congenital amusia: evidence from Cantonese speakers. *Front Hum Neurosci.* 8, 1-
573 19.

574 Lyon, G.R., 1998. Why reading is not a natural process. *Educ Leadersh.* 55, 14-18.

575 Moeller, M.P., White, K.R., Shisler, L., 2006. Primary Care Physicians' Knowledge, Attitudes, and
576 Practices Related to Newborn Hearing Screening. *Pediatrics* 118, 1357-1370.

577 Moller, A., 1999. Neural mechanisms of BAEP. *Electroencephalogr Clin Neurophysiol Suppl.*
578 49, 27-55.

579 Musacchia, G., Sams, M., Skoe, E., Kraus, N., 2007. Musicians Have Enhanced Subcortical
580 Auditory and Audiovisual Processing of Speech and Music. *Proc Natl Acad Sci U S A.* 104,
581 15894–15898.

582 National Institutes of Health, Department of Health and Human Services, National Institute of
583 Child Health and Human Development, 2000. National Reading Panel. Teaching Children
584 to Read: An Evidence-Based Assessment of the Scientific Research Literature on Reading
585 and Its Implications for Reading Instruction. Washington, DC: US Government Printing
586 Office.

587 Neef, N., Schaadt, G., Friederici, A., 2017. Auditory brainstem responses to stop consonants
588 predict literacy. *Clin Neurophysiol.* 128, 484-494.

589 Otto-Meyer, S., Krizman, J., White-Schowoch, T., Kraus, N., 2018. Children with autism spectrum
590 disorder have unstable neural responses to sound. *Exp Brain Res.* 5164-4.

591 Parbery-Clark, A., Anderson, S., Hittner, E., Kraus, N., 2012. Musical experience offsets age-
592 related delays in neural timing. *Neurobiol Aging.* 33, 1483.

593 Parbery-Clark, A., Skoe, E., Kraus, N., 2009. Musical experience limits the degradative effects of
594 background noise on the neural processing of sound. *J Neurosci.* 29, 14100-14107.

595 Russo, N., Nicol, T., Musacchia, G., Kraus, N., 2004. Brainstem responses to speech syllables.
596 *Clin Neurophysiol.* 115, 2021 – 2030.

597 Russo, N., Nicol, T.G., Trommer, B., Zecker, S., Kraus, N., 2009. Brainstem transcription of speech
598 is disrupted in children with autism spectrum disorders. *Dev Sci.* 12, 557–567.

599 Russo, N., Nicol, T.G., Zecker, S.G., Haves, E.A., Kraus, N., 2005. Auditory training improves
600 neural timing in the human brainstem. *Behav Brain Res.* 156, 95-103.

601 Schatschneider, C., Torgesen, J.K., 2004. Using our current understanding of dyslexia to support
602 early identification and intervention. *J Child Neurol.* 19, 759 –765.

603 Skoe, E., Kraus, N., 2010. Auditory brainstem response to complex sounds: a tutorial. *Ear Hear.*
604 31, 302 – 324.

605 Skoe, E., Kraus, N., 2013. Musical training heightens auditory brainstem function during
606 sensitive periods in development. *Front Psychol.* 4, 1-15.

607 Skoe, E., Krizman, J., Anderson, S., Kraus, N., 2013. Stability and plasticity of auditory brainstem
608 function across the lifespan. *Cereb Cortex.* 25, 1415–1426.

609 Skoe, E., Nicol, T., Kraus, N., 2011. Cross-phaseogram: Objective neural index of speech sound
610 differentiation. *J Neurosci Methods.* 196, 308-317.

611 Song, J.H., Skoe, E., Banai, K., Kraus, N., 2012. Training to Improve Hearing Speech in Noise:
612 Biological Mechanisms. *Cereb Cortex.* 22, 1180-1190.

613 Song, J.H., Skoe, E., Wong, P.C., Kraus, N., 2008. Plasticity in the adult human auditory brainstem
614 following short-term linguistic training. *J Cogn Neurosci.* 20, 1892–1902.

615 Strait, D. L., Kraus, N., Skoe, E., Ashley, R., 2009. Musical experience and neural efficiency:
616 effects of training on subcortical processing of vocal expressions of emotion. *Eur J*
617 *Neurosci.* 29, 661–668.

618 Strait, D.L., Kraus, N., 2014. Biological impact of auditory expertise across the life span:
619 musicians as a model of auditory learning. *Hear Res.* 308, 109–121.

620 Strait, D.L., O’Connell, S., Parbery-Clark, A., Kraus, N., 2014. Musicians’ enhanced neural
621 differentiation of speech sounds arises early in life: developmental evidence from ages
622 3 to 30. *Cereb Cortex.* 24, 2512-2521.

623 Strait, D.L., Parbery-Clark, A., Hittner, E., Kraus, N., 2012. Musical training during early childhood
624 enhances the neural encoding of speech in noise. *Brain Lang.* 123, 191–201.

- 625 Strait, D.L., Parbery-Clark, A., O’Connell, S., Kraus, N., 2013. Biological impact of preschool music
626 classes on processing speech in noise. *Dev Cogn Neurosci.* 6, 51-60.
- 627 Stuart, A., Yang, E., Botea, M., 1996. Neonatal auditory brainstem responses recorded from four
628 electrode montages. *J Commun Disord* 29, 125 – 139.
- 629 Stuart, A., Yang, E., Green, W., 1994. Neonatal Auditory Brainstem Response Thresholds to Air-
630 and Bone-Conducted clicks: 0 to 96 Hours Postpartum. *J Am Acad Audiol.* 5, 163 – 172.
- 631 Vellutino, F.R., Fletcher, J.M., Snowling, M.J., Scanlon, D.M., 2004. Specific reading disability
632 (dyslexia): what have we learned in the past four decades? *J Child Psychol Psychiatry.*
633 45, 2– 40.
- 634 Weiss, M.W., Bidelman, G.M., 2015. Listening to the brainstem: musicianship enhances
635 intelligibility of subcortical representations for speech. *J Neurosci.* 35, 1687-1691.
- 636 Welch, P.D., 1967. The use of Fast fourier Transform for the estimation of power spectra: a
637 method based on time averaging over short, modified periodograms. *IEEE Trans.*
638 *Audio Electroacoust.* 15, 70-73.
- 639 White-Schwoch, T., Davies, E.C., Thompson, E.C., Woodruff Carr, K., Nicol, T., Bradlow, A.R.
640 Kraus, N., 2015b. Auditory-neurophysiological responses to speech during early
641 childhood: Effects of background noise. *Hear Res.* 328, 34-47.
- 642 White-Schwoch, T., Kraus, N., 2013. Physiologic discrimination of stop consonants relates to
643 phonological skills in pre-readers: a biomarker for subsequent reading ability? *Front*
644 *Hum Neurosci.* 7, 1-9.
- 645 White-Schwoch, T., Woodruff Carr, K., Thompson, E.C., Anderson, S., Nicol, T., Bradlow,
646 A.R., Zecker, S.G., Kraus, N., 2015a. Auditory processing in noise: A preschool biomarker
647 for literacy. *PLoS Biol.* 13, e1002196.
- 648 Wible, B., Nicol, T., Kraus, N., 2004. Atypical brainstem representation of onset and formant
649 structure of speech sounds in children with language-based learning problems. *Biol*
650 *Psychol.* 67, 299–317.
- 651 Willcutt, E.G., Pennington, B.F., 2000. Psychiatric comorbidity in children and adolescents with
652 reading disability. *J Child Psychol Psychiatry.* 41, 1039 –1048.
- 653 Wong, P.C., Skoe, E., Russo, N.M., Dees, T., Kraus, N., 2007. Musical experience shapes human
654 brainstem encoding of linguistic pitch patterns. *Nat Neurosci.* 10, 420–422.
- 655 Xu, Y., Krishnan, A., Gandour, J.T., 2006. Specificity of experience-dependent pitch
656 representation in the brainstem. *NeuroReport* 17, 1601–1605.
- 657 Zuk, J., Ozernov-Palchik, O., Kim, H., Lakshminarayanan, K., Gabrieli, J.D., Tallal, P., Gaab, N.,
658 2013. Enhanced syllable discrimination thresholds in musicians. *PLoS One* 8: e80546.

659 **Figure legends**

660 **Fig. 1** Distribution of Wave V parameters. Scatter plots depicting all tested newborns (light color
661 filled circles) within box plots for (A) latency, and (B) amplitude. In the scatter plots, dark filled
662 circle and dark filled triangle indicate data corresponding to the individual newborns selected
663 for illustration in successive figures, with high and low SNR respectively. In each box plot, thick
664 black line and black filled diamond indicate the median and mean, respectively.

665 **Fig. 2** Recording setup. Four disposable snap Ag/AgCl electrodes were placed in a vertical
666 montage: the active electrode was located at Fpz (white electrode), references at each ear (red
667 and blue, right and left respectively), and ground electrode at the forehead (black electrode).
668 Only the ipsilateral reference (right electrode) was used in the analysis. The reproduction of the
669 participant's picture is with the written consent of her mother.

670 **Fig. 3** Spectral and temporal neural representation of the syllables /da/ and /ga/ in the
671 newborn's auditory brain. (A) Stimulus waveforms (/da/, /ga/) plotted in black, and grand
672 averaged time-domain FFR waveforms and amplitude FFR spectra extracted from the consonant
673 transition and the vowel stimulus regions to /da/ and /ga/ plotted in red and blue, respectively.
674 (B) Time-domain FFR waveforms and amplitude FFR spectra from an individual newborn with
675 high SNR (NF 029) and (C) from another newborn with low SNR (NF 038).

676 **Fig. 4** Spectrograms from FFRs elicited to syllables /da/ and /ga/. (A) Spectrograms extracted
677 from the grand-averaged FFRs. (B) and (C) spectrograms corresponding to the same individual
678 newborns with high and low SNR depicted in Fig. 3. The color scale from black to white indicates
679 the spectral amplitude in μV , with light colours depicting highest amplitude values (top right).

680 **Fig. 5** Distribution of each of the objective indices retrieved in the time domain. Scatter plots
681 depicting all tested newborns (light color filled circles) within box plots for (A) stimulus-to-
682 response cross-correlation; (B) neural lag; (C) signal-to-noise-ratio (SNR) of the consonant
683 transition and (D) of the vowel; (E) pitch error; and (F) pitch strength measurements to /da/ and
684 /ga/ syllables (depicted in red and blue, respectively). In the scatter plots, dark filled circles and
685 dark filled triangles indicate data corresponding to the individual newborns with high and low
686 SNR, respectively, as depicted in Fig. 3. In each box plot, the thick black line and the black filled
687 diamond indicate the median and mean, respectively.

688 **Fig. 6** Pitch tracking and points below noise floor obtained from (A) the grand average; (B) and
689 (C) obtained from the individual newborns depicted in Fig. 3 with high and low SNR, respectively.
690 F_0 s were extracted separately from the FFRs to /da/ (left column) and /ga/ (right column), as well
691 as from the stimuli (black solid lines) in overlapping steps of 40 ms using an autocorrelation
692 based approach. Light grey areas indicate the bins in which the F_0 spectral amplitude was lower
693 than the F_0 spectral amplitude in the pre-stimulus region (points below noise floor).

694 **Fig. 7** Pitch strength obtained from (A) the grand averaged FFRs; (B) and (C) from the individual
695 newborns depicted in Fig. 3 with high and low SNR, respectively. The figures depict the
696 autocorrelation values (r ; from -1 in black to 1 in white) computed separately from the FFRs to
697 /da/ (left column) and /ga/ (right column) as a function of time and lag. The maximum
698 autocorrelation value per unit of time is marked in black. Notice that the emerging black line is
699 equivalent to the pitch tracking profiles observed in the Fig. 6.

700 **Fig. 8** Distribution of each of the objective indices retrieved in the frequency domain. Scatter
701 plots depicting all tested newborns within box plots for: (A) F_0 and averaged HH_{2-13} spectral

702 amplitudes during the consonant transition, and **(B)** the vowel; and **(C)** points below noise floor
703 measurements, all computed for each syllable separately. The layout is equal to that used in Fig.
704 5.

705

706 **Table 1**

707 Time-domain parameters. Descriptive statistics of stimulus-to-response cross-correlation,
 708 neural lag, RMS amplitude calculated from the pre-stimulus region, SNR computed from the
 709 consonant transition, vowel and entire response, pitch error and pitch strength for each syllable
 710 presented.

711

Measure	/da/ M (SD)	/ga/ M (SD)
Cross-correlation (Pearson's r)	0.15 (0.04)	0.15 (0.03)
Neural lag (ms)	5.87 (1.11)	5.90 (1.16)
Pre-stimulus RMS (μ V)	0.03 (0.01)	0.03 (0.01)
SNR		
<i>Consonant transition (10 – 57 ms)</i>	1.58 (0.75) †	1.82 (0.66)
<i>Vowel (57 – 170 ms)</i>	1.48 (0.41)	1.44 (0.48) †
<i>Entire response (0 – 170 ms)</i>	1.53 (0.44)	1.46 (0.69) †
Pitch error (Hz)	4.89 (2.01)	5.29 (1.78)
Pitch strength (r)	0.61 (0.18)	0.63 (0.17)

712 † Median (IQR, interquartile range)

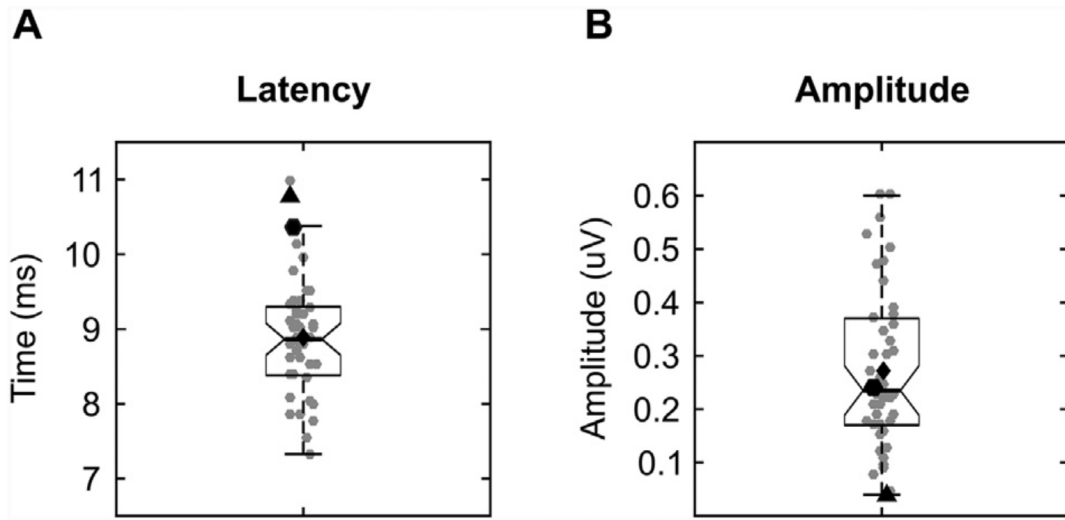
713 **Table 2**

714 Frequency-domain parameters. Descriptive statistics for spectral amplitude across response
 715 syllables, stimulus regions and harmonics and for points below noise floor for each syllable
 716 presented.
 717

Measure	/da/ M (SD)	/ga/ M (SD)
Spectral Amplitude (nV)		
<i>Consonant transition (10 – 57 ms)</i>		
F ₀	40.65 (27.82) †	44.01 (21.45)
HH ₂₋₁₃	3.01 (0.86)	2.52 (0.99) †
<i>Vowel (57 – 170 ms)</i>		
F ₀	35.43 (13.55) †	34.47 (14.42)
HH ₂₋₁₃	2.88 (1.16) †	2.73 (0.66)
<i>Entire response (0 – 170 ms)</i>		
F ₀	38.29 (13.98)	38.11 (14.84)
HH ₂₋₁₃	3.19 (0.89)	2.83 (0.65)
Points below noise floor	2.5 (24.75) †	0 (13.25) †

718 † Median (IQR, interquartile range)
 719
 720

721 **Figure 1**
722

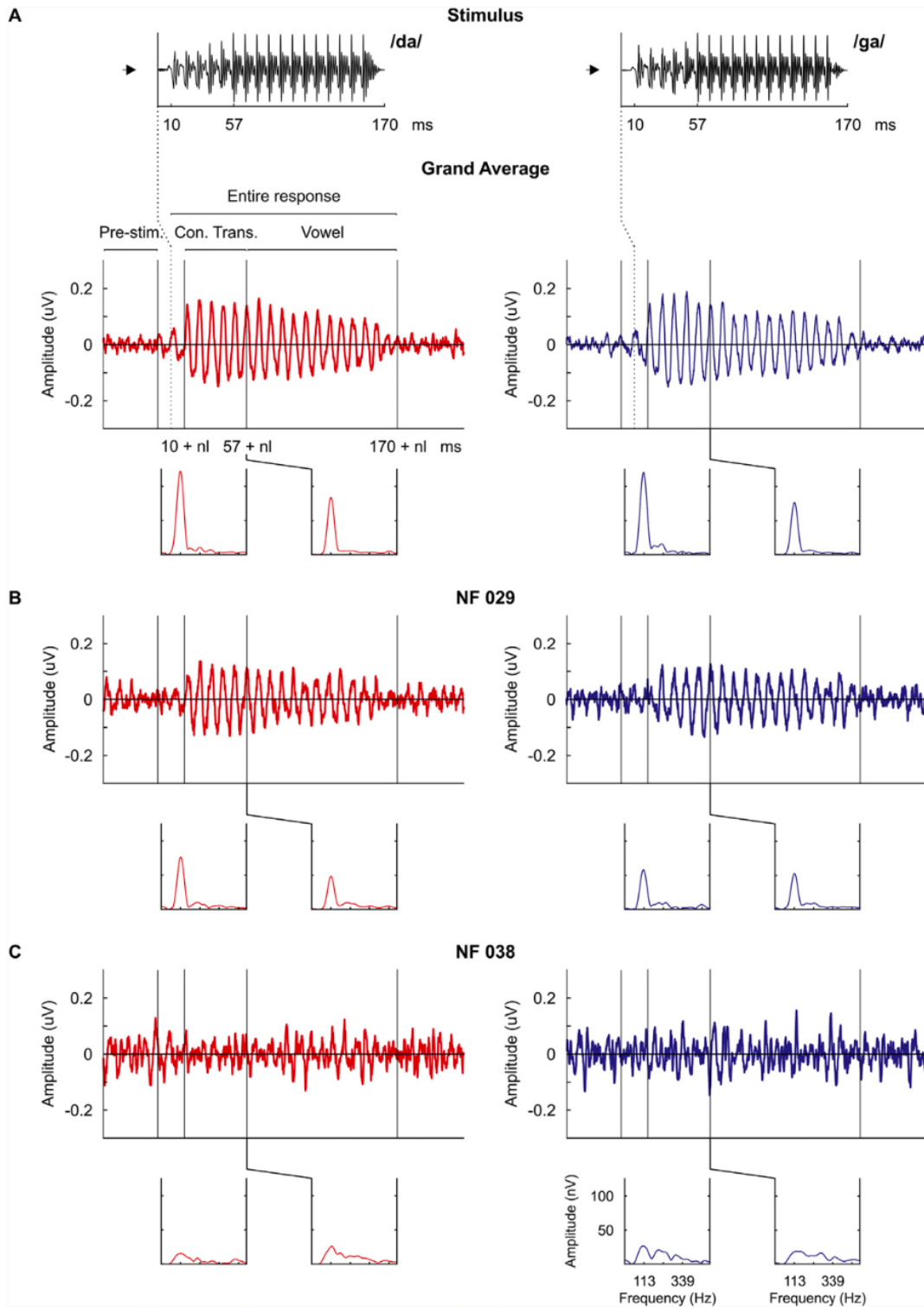


723
724

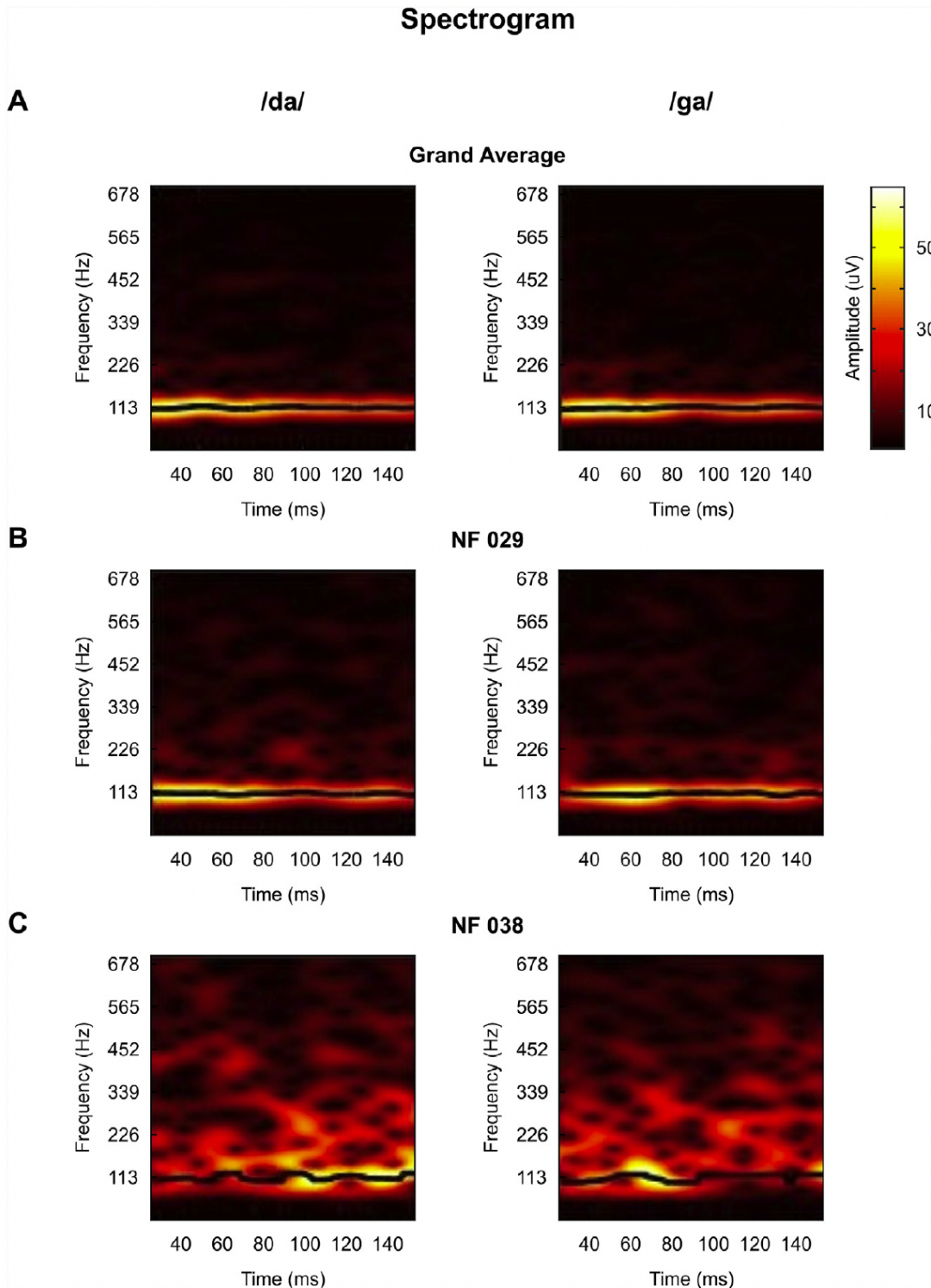
725 **Figure 2**
726



727

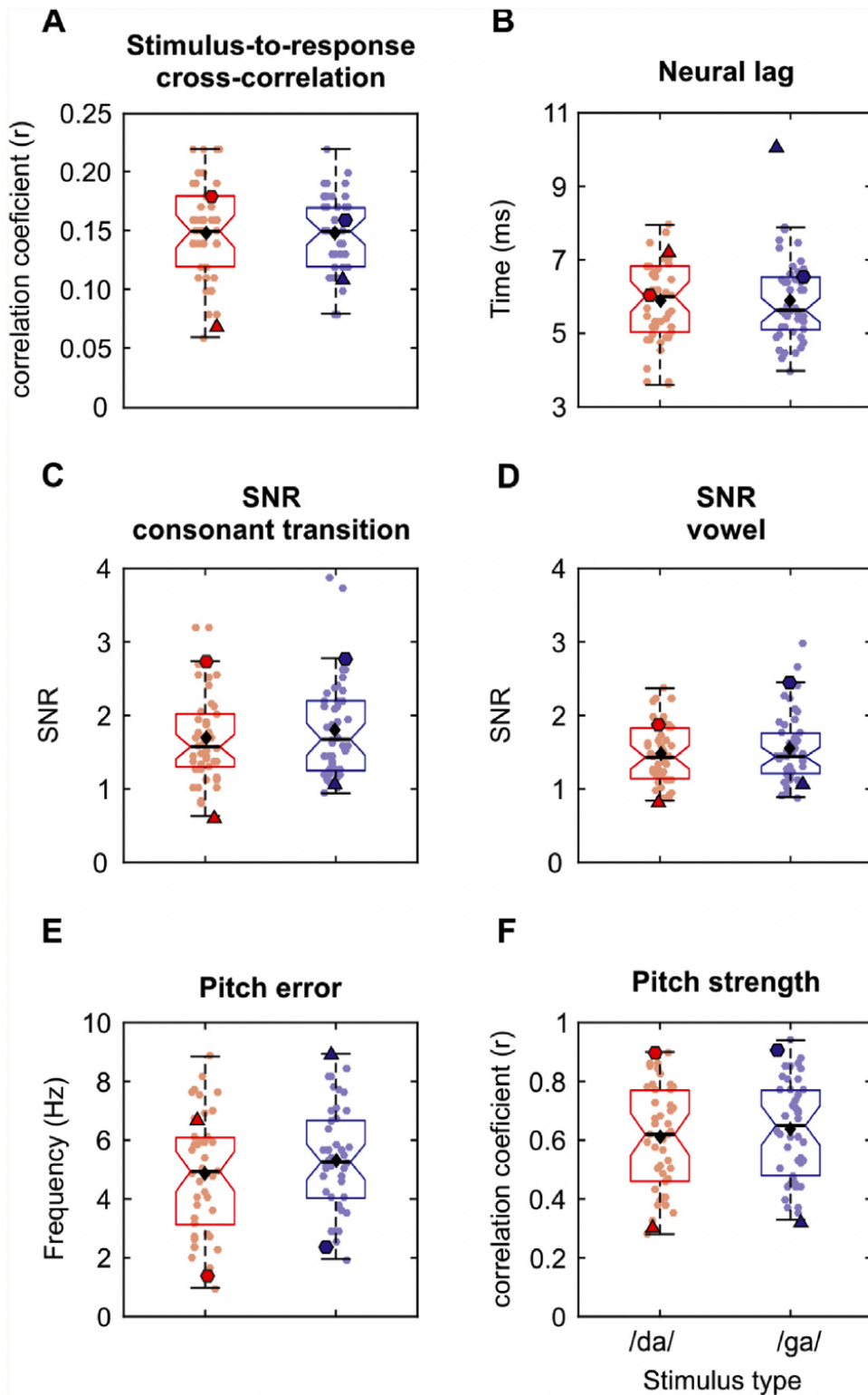


731 **Figure 4**
732

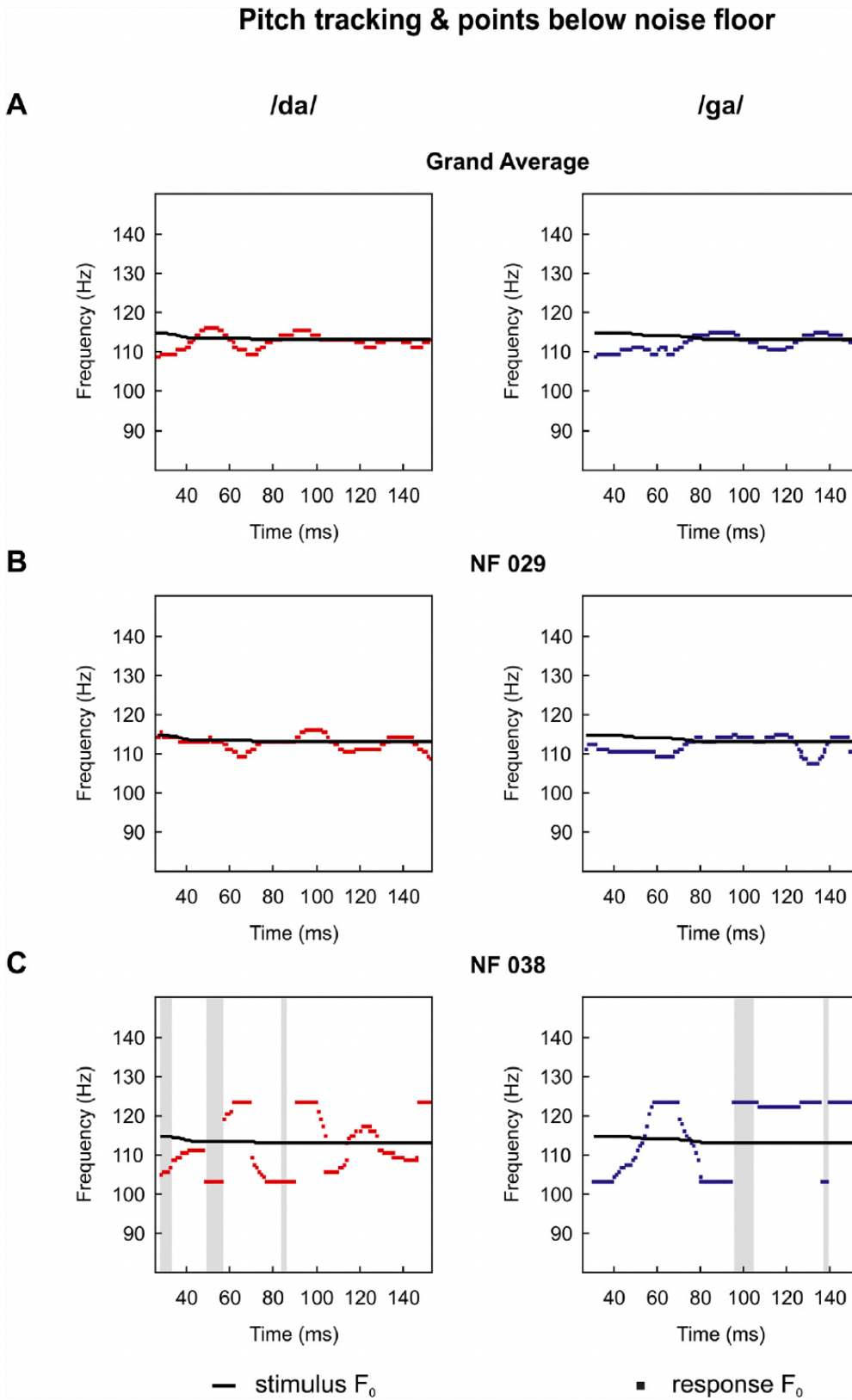


733

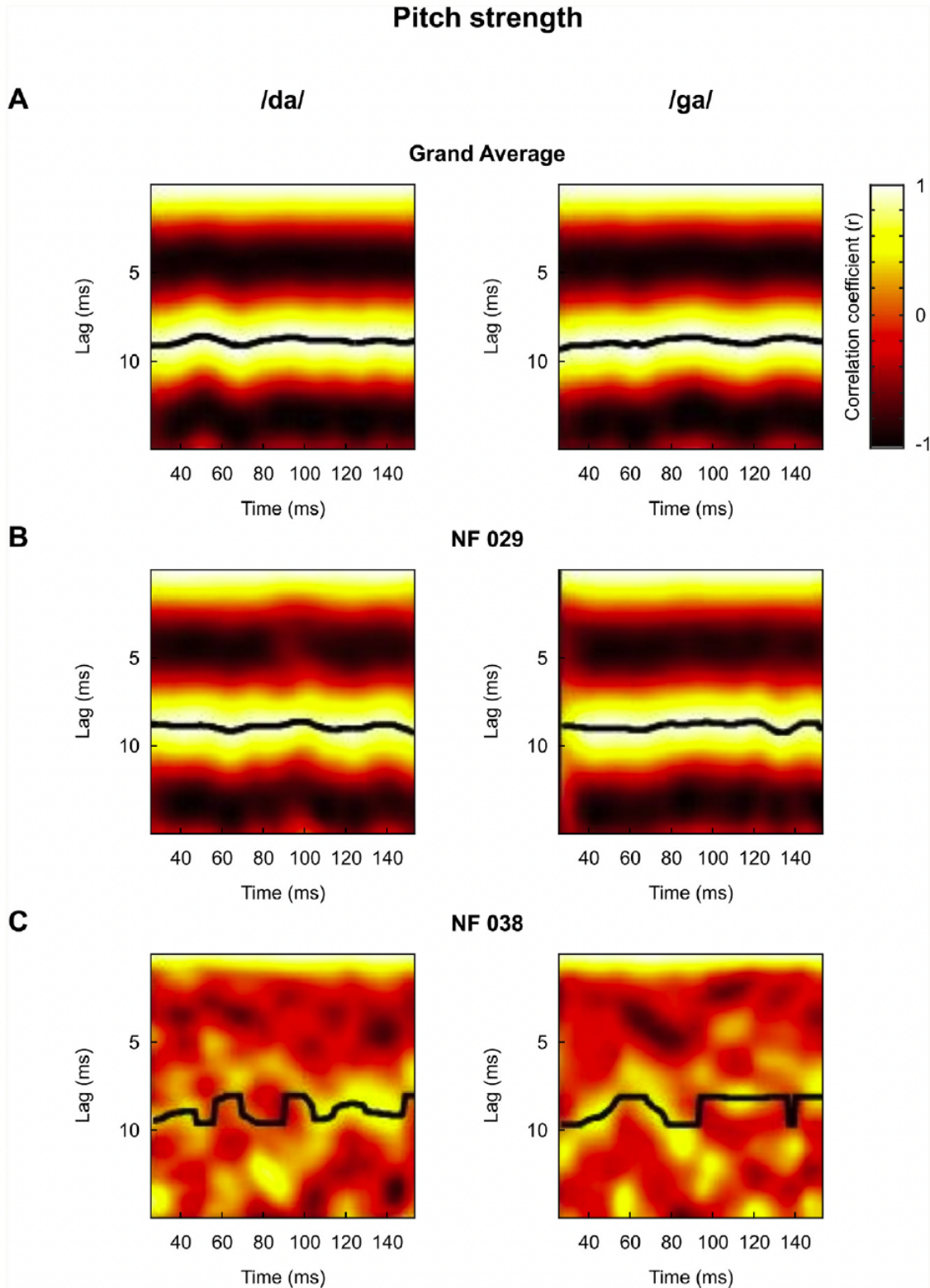
734 Figure 5
735



736
737

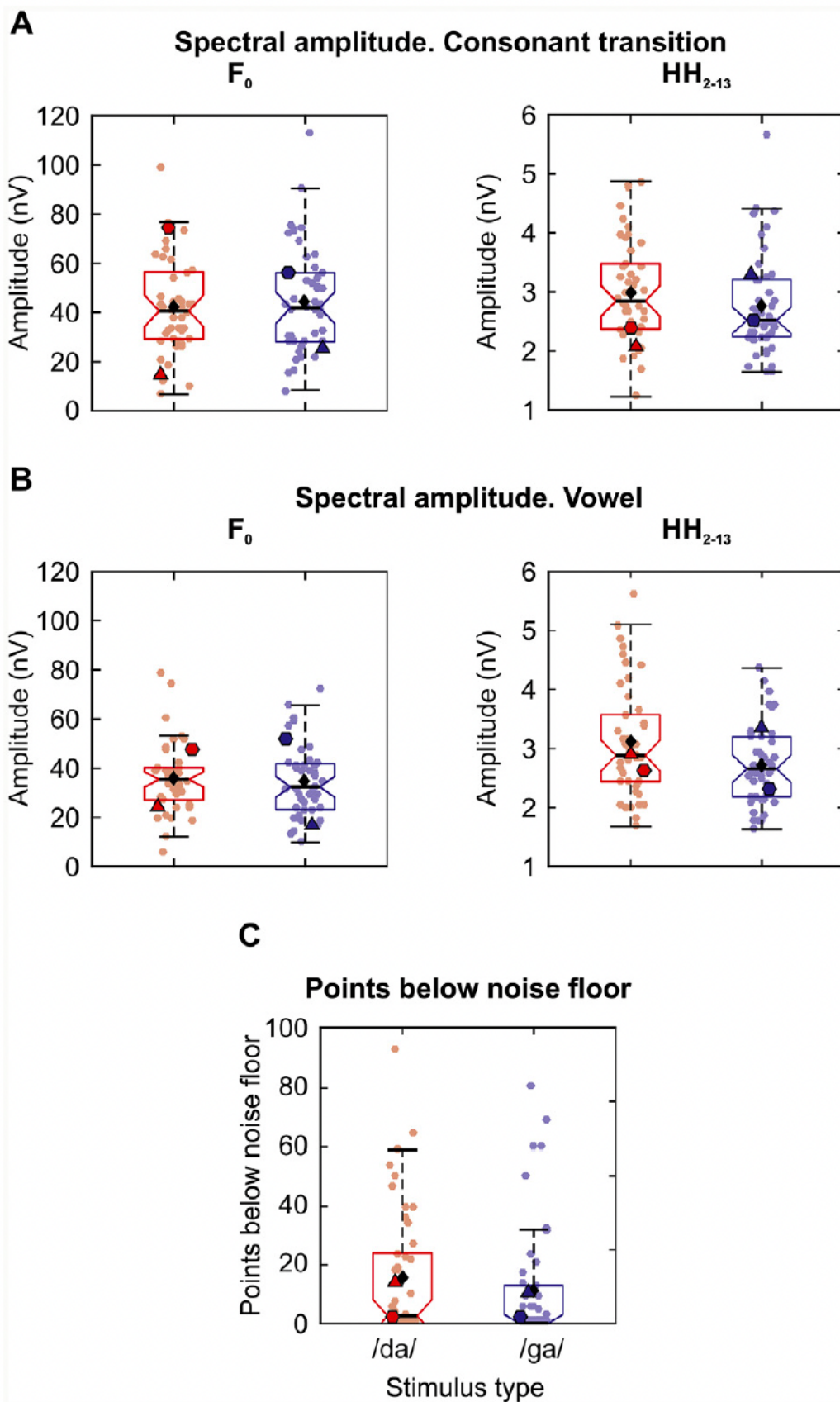


742 **Figure 7**
743



744

745 Figure 8
746



747